



Cite this: *Green Chem.*, 2024, **26**, 8030

Received 26th May 2024,
Accepted 14th June 2024
DOI: 10.1039/d4gc02564d
rsc.li/greenchem

Sustainability in a can: upcycling aluminium scrap in the waste-minimized electrochemical synthesis of 2-oxazoline[†]

Simone Trastulli Colangeli, Francesco Ferlin * and Luigi Vaccaro *

The use and consumption of electrodes is a crucial aspect regarding the overall efficiency and sustainability of electrochemical reactions. When metal electrodes are used, the cost of the material combined with the processing costs assumes relevance in terms of economics and sustainability. Herein we report a case study that aims to define an electrochemical synthetic protocol using electrodes prepared from recovered aluminium scrap. We approached the problem by evaluating and comparing the different carbon footprints associated with the use of different electrode materials from primary sources and secondary (recycled) sources. We optimized the use of electrodes made from secondary aluminium to develop a simple, oxidant-free protocol for the representative synthesis of 2-oxazolines from amino alcohols and aldehydes using generally elusive concentrated conditions and a recoverable reaction media. A further evaluation of the developed process using green metrics allowed us to quantify the waste distribution of our procedure in comparison with the literature processes as well as the progress in terms of sustainability and intrinsic reaction efficiency.

Introduction

To limit global warming, carbon neutrality is becoming an increasingly urgent challenge.¹ The decarbonization of the chemical industry is of particular strategic importance as it is responsible for 15% of global industrial greenhouse gas (GHG) emissions.² In this context, electrochemical production based on the use of electricity from renewable sources is becoming a promising alternative to reduce the carbon footprint of chemicals.³ While research on the use of electrolytic processes for the production of green hydrogen and CO₂ reduction is expanding, electrochemical industrial processes are so far mainly limited to the chlor-alkali and aluminium sectors.⁴

To succeed in the challenging application of electrochemistry in industrial chemical synthesis, researchers are focusing their efforts on optimizing key process parameters such as energy efficiency, product selectivity, productivity per time unit, and electrocatalyst efficiency.⁵

The consumption of electrodes represents a key aspect influencing the efficiency and sustainability of electrosynthesis.

Laboratory of Green S.O.C. – Dipartimento di Chimica, Biologia e Biotecnologie, Università degli Studi di Perugia, Via Elce di Sotto 8, 06123 – Perugia, Italy.
E-mail: luigi.vaccaro@unipg.it; greensoc.chm.unipg.it

[†] Electronic supplementary information (ESI) available: General procedures, full characterization of the synthesized compounds and copies of ¹H, ¹³C and ¹⁹F NMR spectra. See DOI: <https://doi.org/10.1039/d4gc02564d>

For example, in the case of the Hall-Héroult process that uses non-metallic electrodes for aluminium smelting, about 400 kg of carbon anode are consumed per ton of aluminium produced.⁷ When electrodes are based on metals, their cost and preparation are even more critical, and it is not easy to generalize information on the electrode consumption. For example, in the electrocoagulation processes employed in wastewater treatment, the aluminium consumption rate is approximately 2 kg per kg of contaminant removed.⁸

While research on finding durable and stable electrodes is extensive, more emphasis should be placed on using electrodes made from waste materials.⁹ This can be even more crucial considering the availability of metallic materials compared to polymers.¹⁰

Aluminium, while being widely used in electrochemistry, is currently included in the list of critical raw materials and is classified as “primary” or “secondary”.

Primary aluminium is derived directly from bauxite, while secondary aluminium is derived from the recycling of primary aluminium.¹¹ The production of secondary aluminium is a more sustainable access route to this metal as its energy cost is only 5% of that of the primary production, and in addition, it includes the advantage of reducing the waste and the consumption of bauxite.¹² In fact, recycling and upcycling are fundamental methodologies in a circular economy strategy that allows more sustainable access to the desired materials while



making the process more ready to be integrated into modern production principles.¹³

In this contribution, we report our study aimed at the definition of novel electrochemical synthetic protocols employing electrodes prepared from recovered scrap aluminium. In coherence with our circular-economy approach to the definition of effective synthetic methodologies,¹⁴ we have prepared electrodes from aluminium can waste. We have therefore optimized their use to develop a simple, oxidant-free protocol for the representative synthesis of 2-oxazolines starting from amino alcohols and aldehydes. To confirm the validity of our approach, we compared the different carbon footprints associated with the use of different electrodes. Finally, we decided to prove the practical utility of our methodology we have also reported a larger-scale synthesis and the preparation of chiral PyOX ligand.

We have decided to test our aluminium can waste-derived electrodes in the synthesis of 2-oxazoline as this process is of general representative interest and this class of compounds find application in several different areas.¹⁵

Generally, 2-oxazolines are prepared by (A) reactions between an amino alcohol and a nitrile or carboxylic acid using various catalysts in combination with heat or MW irradiation;¹⁶ (B) the coupling between an amino alcohol and an aldehyde using a chemical oxidant, *i.e.* molecular iodine in combination of heat and bases, hydrobromide perbromide (PHPB), diacetoxyiodobenzene (PIDA) or *N*-bromosuccinimide (NBS).¹⁷

Electrochemistry offers an intriguing opportunity to replace chemical oxidants with electrons. Different well established electrochemical protocols based on the oxidative cyclization of β -amino arylketones or olefinic amides (Fig. 1).¹⁸ Anyway a direct electrochemical approach between an amino alcohol and an aldehyde is not reported.

Results and discussion

We began our investigation by employing 4-fluorobenzaldehyde **1a** and ethanolamine **2** as model substrates to optimize the best reaction conditions. We found that product **3a** was obtained in 88% isolated yield (Table 1, entry 1) using LiBr as supporting electrolyte, graphite anode and aluminium cathode in an undivided cell at 50 mA, after the passage of 7 F mol⁻¹ of charge (Faraday efficiency equal to 27%). The reaction medium influences the efficiency of the process and the best results were achieved in a mixture of methanol:acetonitrile (1 : 1) (entry 1) while changing the solvent to methanol, acetonitrile, ethanol, or water conversions decreased (Table 1, entries 2–5).

It is noteworthy that in our conditions, the use of stoichiometric amounts of **1a** and **2** is functional for achieving best results. Increasing the amount of **2**, leads to poorer conversions (Table 1, entries 6 and 7). Without using bromide salts as electrolytes, the reaction does not proceed satisfactorily, suggesting that electrolyte participates in the mechanism as a redox mediator (Table 1, entries 8–11). Finally, by performing the process with no current, product **3a** was not observed at all (Table 1, entry 12).

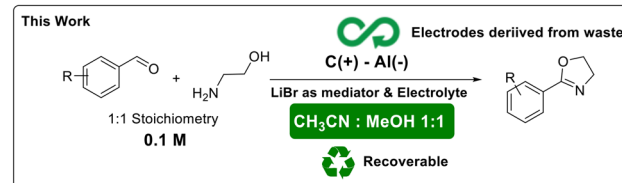
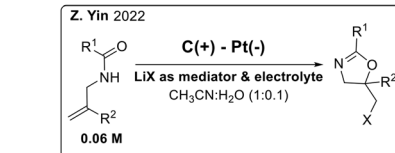
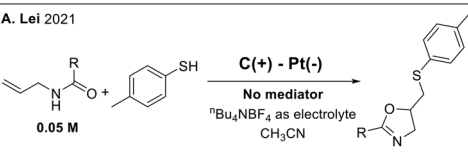
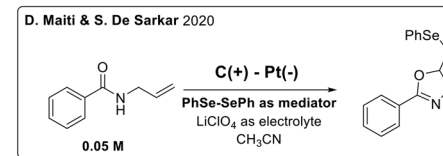
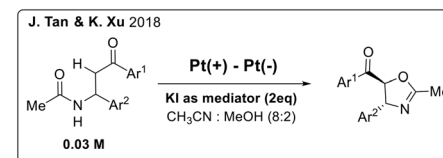


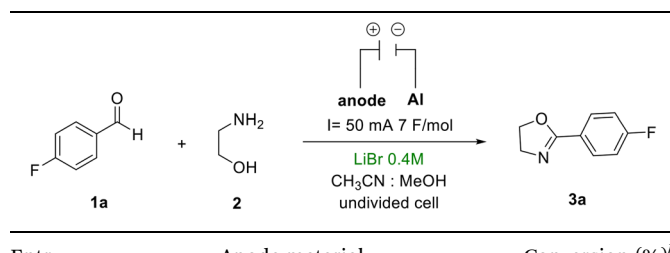
Fig. 1 Known approaches to the electrosynthesis of 2-oxazolines.

Table 1 Solvent and supporting electrolyte optimization^a

Entry	Solvent	Supporting electr.	Conversion ^b (%)	Reaction conditions	
				I = 50 mA 7 F/mol	Supp. Electr. 0.4 M solvent 0.1 M undivided cell
1	CH ₃ CN : MeOH 1 : 1	LiBr	93 (88)		
2	MeOH	LiBr	61		
3	CH ₃ CN	LiBr	0		
4	EtOH	LiBr	31		
5	H ₂ O	LiBr	5		
6 ^c	CH ₃ CN : MeOH 1 : 1	LiBr	84		
7 ^d	CH ₃ CN : MeOH 1 : 1	LiBr	62		
8	CH ₃ CN : MeOH 1 : 1	KBr	56		
9	CH ₃ CN : MeOH 1 : 1	<i>n</i> Bu ₄ NPF ₆	0		
10	CH ₃ CN : MeOH 1 : 1	NaI	5		
11	CH ₃ CN : MeOH 1 : 1	KPF ₆	0		
12 ^e	CH ₃ CN : MeOH 1 : 1	LiBr	0		

^a Reaction conditions: **1a** (0.5 mmol), **2** (0.5 mmol), supporting electrolyte (0.4 M), solvent (5 mL, 0.1 M), graphite anode and aluminium cathode, 50 mA of current for 7 F mol⁻¹ of charge based on **1a** (about 110 minutes) at 25 °C. ^b GLC conversion has been determined using samples of pure compound as reference standards; the remaining materials are **1a** and **2**, isolated yield in parenthesis. ^c 2 equivalents of **2** were used. ^d 4 equivalents of **2** were used. ^e Without current.



Table 2 Anode material optimization table^a

Entry	Anode material	Conversion (%) ^b
1	Graphite	93
2	Stainless steel	0
3	Copper	0
4	Zinc	0

^a Reaction conditions: **1a** (0.5 mmol), **2** (0.5 mmol), LiBr (0.4 M) as supporting electrolyte, CH₃CN : CH₃OH (1 : 1, 5 mL) as solvent, aluminium cathode, 50 mA of current for 7 F mol⁻¹ of charge based on **1a** (about 110 minutes) at 25 °C. ^b GLC conversion has been determined using samples of pure compound as reference standards; the remaining materials are **1a** and **2**, isolated yield in parenthesis.

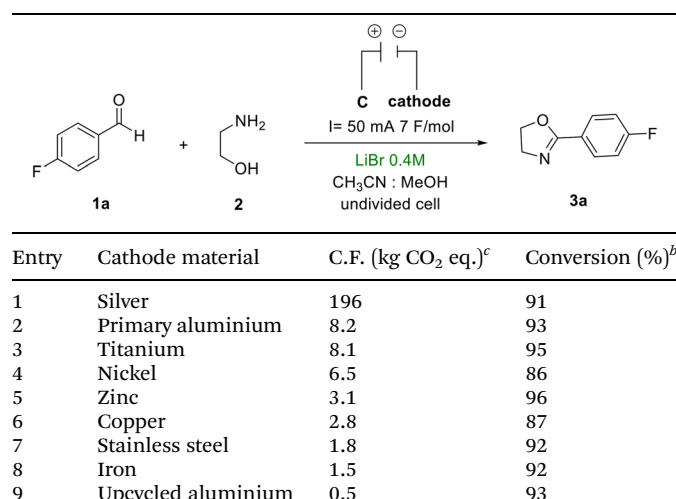
Investigation continued to compare different materials for the electrodes. In Table 2 are shown the results that confirm how important is the use of graphite anode. This behaviour indicates that probably, among the materials tested, graphite has the least overpotential towards bromide oxidation. On the other hand, different metallic cathodes were selected, taking into consideration the carbon footprint associated with the different materials. Carbon footprint, measured in kg CO₂ equivalent per kg of product, is an intuitive parameter that measures the quantity of CO₂ emitted in the entire production cycle of the material of interest.¹⁹

From the data reported in Table 3, we can see that the efficiency of the reaction remains almost constant while varying the cathode materials. Based on this evidence, we could focus on cathode materials with the lowest environmental impact and lowest carbon footprint. Aluminium is on the list of critical raw materials, but it is also highly recyclable.¹³

Based on the 2021 Climate Action report,²⁰ post-consumer aluminium scrap has an associated carbon footprint of about 0.5 kg CO₂ per kg of aluminium that is related to its collection, transport, and smelting.²⁰ Additionally, it should be mentioned that recovered post-consumer aluminium scrap leads to a lower purity product, often unattractive for most markets that instead prefer to use higher purity materials.²¹

For all these reasons, we have decided to focus on using aluminium from recovered cans as cathode material. Recovered cans were used without any further manipulation, as the cathode gave an excellent 93% conversion to **3a** and confirmed the effective use of this highly interesting source of aluminium from post-consumer scrap (Table 3, entry 9).

At this stage, we also investigated the possibility of recovering the acetonitrile/methanol mixture used as reaction medium. Due to their similarity, their direct evaporation allowed us to recover 80% of the original 1 : 1 ACN : MeOH mixture (as confirmed by ¹H-NMR). Encouraged by these results, we next decided to demonstrate the synthetic utility

Table 3 Cathode material optimization table & associated carbon footprint^a

Entry	Cathode material	C.F. (kg CO ₂ eq.) ^c	Conversion (%) ^b
1	Silver	196	91
2	Primary aluminium	8.2	93
3	Titanium	8.1	95
4	Nickel	6.5	86
5	Zinc	3.1	96
6	Copper	2.8	87
7	Stainless steel	1.8	92
8	Iron	1.5	92
9	Upcycled aluminium	0.5	93

^a Reaction conditions: **1a** (0.5 mmol), **2** (0.5 mmol), LiBr (0.4 M) as supporting electrolyte, CH₃CN : CH₃OH (1 : 1, 5 mL) as solvent, graphite anode, 50 mA of current for 7 F mol⁻¹ of charge based on **1a** (about 110 minutes) at 25 °C, cathode material as described in the Table 3.

^b GLC conversion has been determined using samples of pure compound as reference standards; the remaining materials are **1a** and **2**.

^c Carbon footprint associated with the production of different pure metals²² and stainless steel.²³

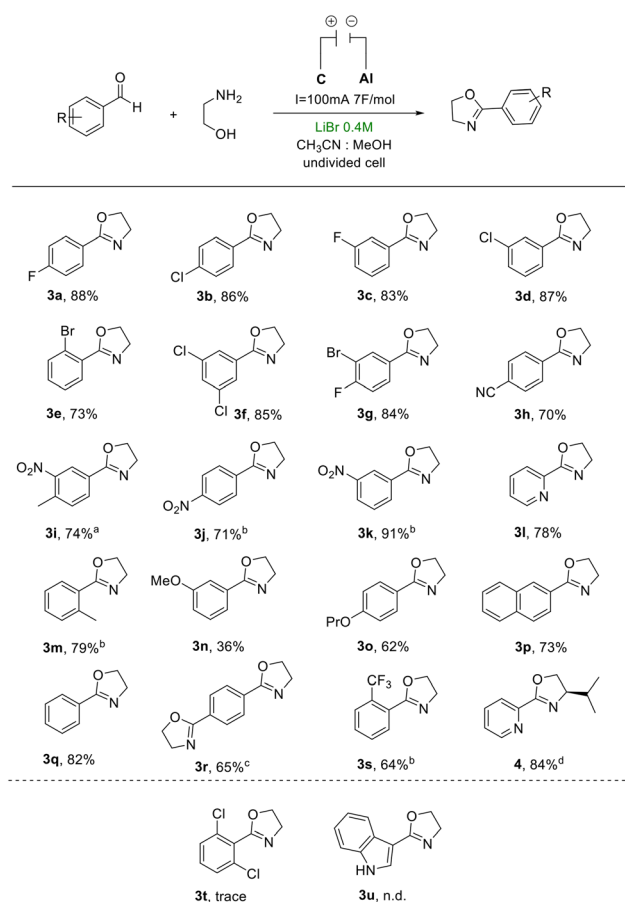
and tolerability of our protocol, exploring the scope of various substrates (Scheme 1).

In general, substrates featuring electron-withdrawing substituents led to high yields with a faraday efficiency equal to. By using halogen-substituted benzaldehydes in the *para* (**2a**, **2b**), *meta* (**2c**, **2d**) or *ortho* (**2e**) positions, products **3** were obtained satisfactory yields. Also, halogen poly-substituted rings (**2f**, **2g**) show similar good results, making the procedure quite interesting for the post-functionalization of substrates by cross-coupling reactions. Other electron-withdrawing groups, such as cyano (**2h**), nitro (**2i**, **2j**, **2k**) or pyridyl (**2l**), lead to high yields of the corresponding products **3** as well. However, nitro-substituted benzaldehydes required a longer reaction time (8 F mol⁻¹, *ca.* 130 minutes).

Electron-donor substituents showed lower efficiency. *ortho*-Tolualdehyde (**2m**) and *ortho*-trifluoromethylbenzaldehyde (**2s**) required longer reaction time, probably due to the steric hindrance effect. *meta*-substitution with methoxy group (**2n**) drastically decreases the yield in **3n**. However, the propoxy group in *para* position (**2o**) led to a good, isolated yield. Concerning the product of terephthaldehyde (**2r**), it was not possible to steer the reaction towards the formation of the mono-oxazoline product using less amount of ethanolamine. We assume that the higher reactivity of the mono-oxazoline product compared to terephthaldehyde is due to electronic effects, making the procedure ineffective for the formation of aldehydes-substituted oxazolines.

It worthy to notice that with our procedure, we successfully synthesized a chiral ligand of the PyOX type (**4**), that has been used in various nickel, iridium, copper or palladium-catalyzed

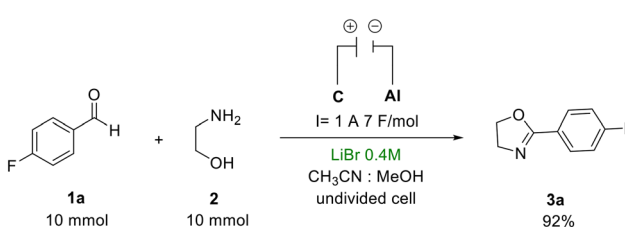




Scheme 1 Scope of the electrochemical synthesis of oxazoline.
^a Reaction conditions: **1a** (1 mmol), **2** (1 mmol), LiBr (0.4 M) as supporting electrolyte, $\text{CH}_3\text{CN} : \text{CH}_3\text{OH}$ (1 : 1, 10 mL) as solvent, graphite anode and aluminum cathode, 100 mA of current for 7 F mol^{-1} of charge based on **1a** (about 110 minutes). All reported yields are isolated yields. ^b 8 F mol^{-1} of charge passed (about 130 minutes). ^c 2 equivalents of ethanolamine (**2**) and 12 F mol^{-1} of charge passed (about 190 minutes). ^d (*S*)-2-Amino-3-methylbutan-1-ol (**2a**) was used instead of ethanolamine (**2**).

reactions.²⁴ Product **4** could be isolated in 84% yield and 95% *ee*, therefore preserving the enantiopurity of the starting material. Substrates **2t** and **2u**, let to unsuccessful results presumably due to steric and electronic effects (Scheme 1). In addition, a gram-scale test was also performed showing that scalability of our synthetic protocol is possible (Scheme 2).

Interestingly, under such slightly larger scale conditions, solvent distillation was expectedly more effective with 87% of the initial mass recovered.



Scheme 2 Large scale electrochemical synthesis of **3a**.

Finally, to quantify the advances in terms of chemical and environmental efficiency, we calculated different green metrics for our electrochemical approach (*E*-factor, Reaction Mass Efficiency (RME), and Material Recovery Parameter (MRP)), and for some of the common procedures reported in the literature²⁵ (Scheme 3). We compared seven different protocols that varied in nature of the process (intramolecular or intermolecular), mechanism (oxidative or reductive), solvent and additives. From the data reported Scheme 3 and ESI,[†] we can confirm the advances in terms of sustainability of our protocol.

The *E*-factor distribution analysis (see ESI[†] for complete details of the percentages) shows that, in the gram-scale procedure, recovering the reaction mixture and avoiding the use of a chemical oxidant led to an *E*-factor as low as 18.7, value that derives only from the mass of non-recovered solvent, with a minor contribution of the excess of LiBr. On the contrary, most of the compared literature processes require tedious and wasteful work-up procedures to remove oxidant, reductant or their byproducts and obviously result strongly in larger total *E*-factor values (range 84.4–465.7).

Reaction mass efficiency (RME) for our protocol is 5.1% (3.7% for the one-mmol scale), while other procedures never exceed an RME value of 1.2%, with most of them falling in the range of 0.2–0.6%.

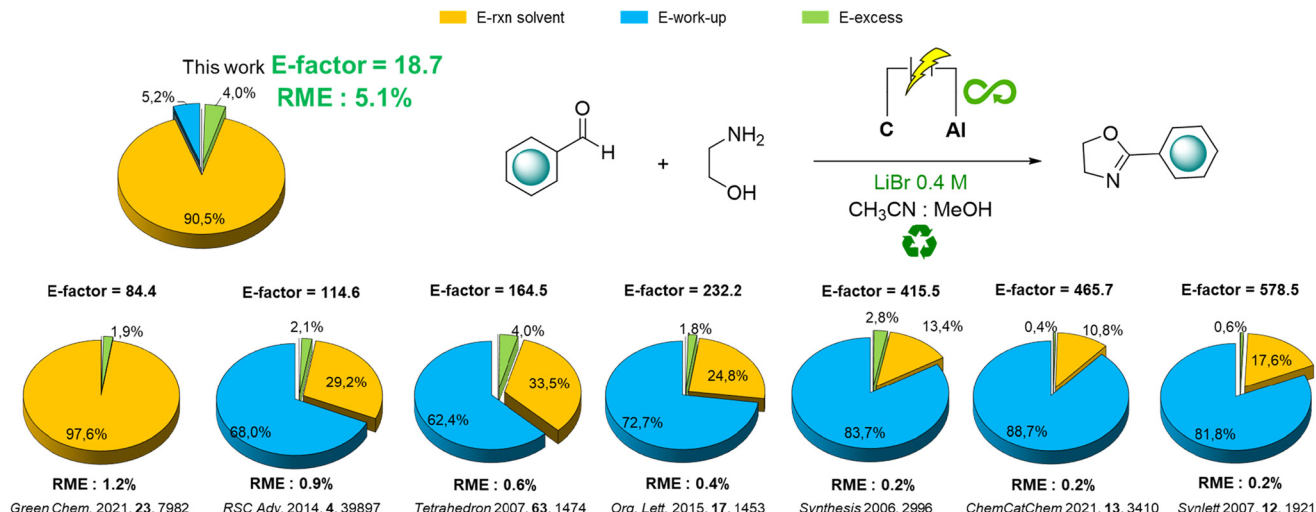
To conclude this study, we have decided to have more insights into the reaction mechanism, and therefore, some control experiments were conducted (Scheme 4). First, the reaction was carried out without electrolysis in the presence of 4 equivalents of molecular bromine, but the reaction did not proceed at all. Nevertheless, using 4 equivalents of Br₂ in combination with 1 equivalent of lithium methoxide led to the formation of **3a** in 52% yield after 2 hours, demonstrating the key role of the base.

No product formation was observed when the reaction was performed in the presence of 1 equivalent of TEMPO, therefore suggesting a radical-type reaction pathway.

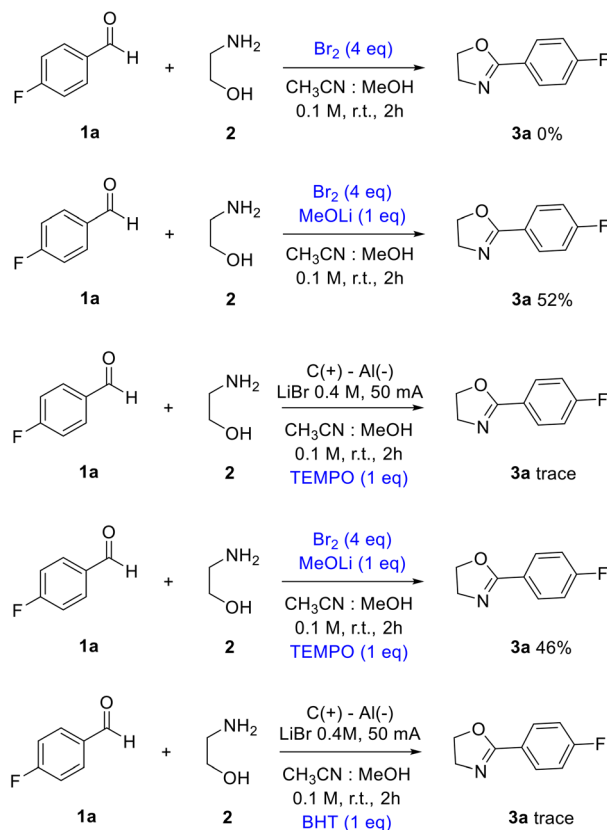
Performing the reaction without electrochemical conditions and using molecular bromine/lithium methoxide but in the presence of 1 equivalent of TEMPO, the reaction proceeds anyway without significant variation in conversion or yield. Therefore, this allowed to conclude that the traditional chemical conditions an anionic reaction pathway is operative.

By performing the electrochemical reaction in presence of 1 equivalent of BHT, product **3a** was not observed. These results together with the fact that electrolysis does not lead to product formation in the absence of bromide salts, suggest that the reaction proceed *via* halogen radicals rather than through a simple hydrogen atom transfer (HAT) pathway.

Furthermore, a cyclic voltammetry analysis was conducted (Fig. 2). As it can be seen from these measurements, the oxidation peak doesn't change in the case of lithium bromide alone (upper chart) or in the presence of reagents **1a** and **2** (bottom chart). The oxidation peak occurs around 0.95 V *vs.* Ag/AgNO₃ reference electrode and no appreciable catalytic current is observed upon the addition of substrates. This

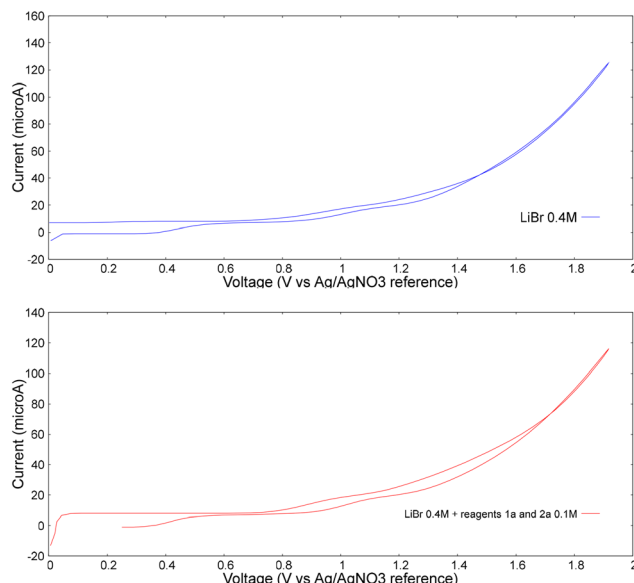


Scheme 3 Sustainability assessment and comparison.



Scheme 4 Control experiment for the electrochemical synthesis of 3a.

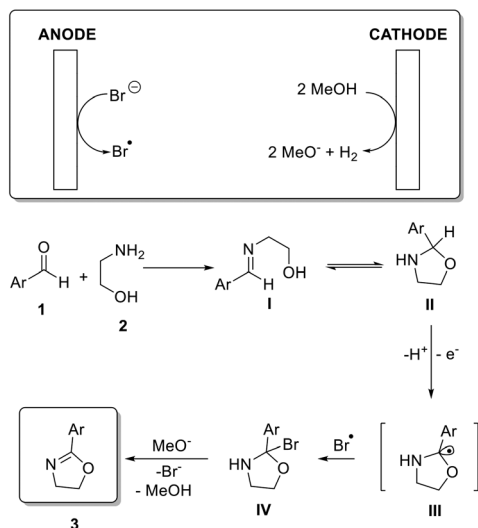
experimental observation leads to the conclusion that when graphite is used as anode, only bromide undergoes oxidation, suggesting its ability to mediate the oxidation of substrate. Based on the control experiments and on the data reported in literature, the plausible mechanism is described in Scheme 5. First, benzaldehyde undergoes a nucleophilic attack by

Fig. 2 Cyclic voltammetry experiments: upper chart: LiBr 0.4 M, MeCN:MeOH 1:1, sweep 200 mV s⁻¹; lower chart: LiBr 0.4 M, 1a 0.1 M, 2 0.1 M, MeCN:MeOH 1:1, sweep 200 mV s⁻¹.

ethanolamine, giving the imine condensation product **I** by eliminating a molecule of water.

Species **I** tautomerizes to oxazolidine **II** that is oxidized to **III** with an electron loss by halogen radical induced process. The radical-radical coupling between **III** and radical bromine furnish **IV**, which, after subsequent base-mediated elimination, gives final 2-oxazoline product **3**. From the substrate scope we can highlight that: (1) benzaldehydes with electron-withdrawing groups give better yields; (2) benzaldehydes with *ortho* substituents give slower reactions. These considerations suggest that the most probable rate-limiting step is the formation of the imine **I**.





Scheme 5 Plausible reaction mechanism.

Conclusions

In conclusion, we have developed an electrochemical approach to synthesize 2-oxazoline **3a–s** and **4** with a broad range of substitutions, starting from inexpensive and commercially available starting materials, also on a gram-scale. The reaction was carried out using cheap electrode materials, in particular, using cathode deriving from aluminium scrap. The utilization of electrodes made by post-consumer aluminium cans has also allowed to minimize the carbon footprint for making effective electrodes. Control experiments were performed to elucidate the reaction mechanism. Finally, a sustainability assessment using green metrics allowed to quantify the advances in terms of sustainability and the inherent environmental efficiency and potential of the electrochemical approach reported.

Author contributions

The manuscript was written through the contributions of all authors. All authors have given approval to the final version of the manuscript. S. T. C.: investigation, methodology, data analysis, manuscript preparation; F. F. and L. V.: conceptualization, project administration, manuscript review/editing.

Conflicts of interest

There are no conflicts to declare.

Acknowledgements

This work has been funded by the European Union – NextGenerationEU under the Italian Ministry of University and Research (MUR) National Innovation Ecosystem grant

ECS000000041 – VITALITY. We acknowledge Università degli Studi di Perugia and MUR for support within the project Vitality. MUR is also thanked for PRIN-PNRR 2022 project “P2022XKWH7 – CircularWaste”.

References

- (a) L. De La Peña, R. Guo, X. Cao, X. Ni and W. Zhang, *Resour., Conserv. Recycl.*, 2022, **177**, 105957; (b) A. Elshkaki and L. Shen, *Energies*, 2022, **15**, 4967.
- M. H. Barecka and J. W. Ager, *Energy Adv.*, 2023, **2**, 268–279.
- (a) D. S. Mallapragada, Y. Dvorkin, M. A. Modestino, D. V. Esposito, W. A. Smith, B.-M. Hodge, M. P. Harold, V. M. Donnelly, A. Nuz, C. Bloomquist, K. Baker, L. C. Grabow, Y. Yan, N. N. Rajput, R. L. Hartman, E. J. Biddinger, E. S. Aydil and A. D. Taylor, *Joule*, 2023, **7**, 23–41; (b) R. Xia, S. Overa and F. Jiao, *JACS Au*, 2022, **2**, 1054–1070; (c) Z. J. Schiffer and K. Manthiram, *Joule*, 2017, **1**, 10–11.
- (a) M. Ostadi, K. G. Paso, S. Rodriguez-Fabia, L. E. Øi, F. Manenti and M. Hillestad, *Energies*, 2020, **13**, 4859; (b) M.-Y. Lee, K. T. Park, W. Lee, H. Lim, Y. Kwon and S. Kang, *Crit. Rev. Environ. Sci. Technol.*, 2019, **50**, 769–815; (c) G. G. Botte, *Electrochem. Soc. Interface*, 2014, **23**, 49–55.
- (a) T. Noël, Y. Cao and G. Laudadio, *Acc. Chem. Res.*, 2019, **52**, 2858–2869; (b) N. Tanbouza, T. Ollevier and K. Lam, *iScience*, 2020, **23**, 101720.
- M. Moradi, Y. Vasseghian, A. Khataee, M. Koby, H. Arabzade and E.-N. Dragoi, *J. Ind. Eng. Chem.*, 2020, **87**, 18–39.
- (a) S. K. Padamata, K. Singh, G. M. Haarberg and G. Saevarsottir, *J. Electrochem. Soc.*, 2023, **170**, 073501; (b) A. T. Tabereaux and R. D. Peterson, *Treatise Process Metall.*, 2014, 839–917.
- (a) A. Arabameri, M. R. Alavi Moghaddam, A. R. Azadmehr and M. Payami Shabestari, *Chem. Eng. Process.*, 2022, **174**, 108869; (b) M. A. Sadik, *Adv. Chem. Eng. Sci.*, 2019, **09**, 109–126; (c) D. T. Moussa, M. H. El-Naas, M. Nasser and M. J. Al-Marri, *J. Environ. Manage.*, 2017, **186**, 24–41.
- (a) N. Iduṣuyi, O. O. Ajide, R. Abu, O. A. Okewole and O. O. Ibiyemi, *Mater. Today: Proc.*, 2022, **56**, 1712–1716; (b) M. Moradi, Y. Vasseghian, A. Khataee, M. Koby, H. Arabzade and E.-N. Dragoi, *J. Ind. Eng.*, 2020, **87**, 18–39.
- S. Du, S. Zhang, J. Wang, Z. Lv, Z. Xu, C. Liu, J. Liu and B. Liu, *J. Cleaner Prod.*, 2024, 141176.
- G. Wallace, *Fundamentals of Aluminium Metallurgy*, 2011, pp. 70–82.
- https://rmis.jrc.ec.europa.eu/uploads/CRM_2020_Factsheets_critical_Final.pdf.
- (a) J. Cho, B. Kim, T. Kwon, K. Lee and S.-I. Choi, *Green Chem.*, 2023, **25**, 8444–8458; (b) Z. Yu, Y. J. Lim, T. Williams and S. Nutt, *Green Chem.*, 2023, **25**, 7058–7061; (c) Y. Wang, K. Liu, F. Liu, C. Liu, R. Shi and Y. Chen, *Green Chem.*, 2023, **25**, 5872–5877.



14 (a) F. Ferlin, F. Valentini, D. Sciosci, M. Calamante, E. Petricci and L. Vaccaro, *ACS Sustainable Chem. Eng.*, 2021, **9**, 12196–12204; (b) F. Valentini, F. Ferlin, S. Lilli, A. Marrocchi, L. Ping, Y. Gu and L. Vaccaro, *Green Chem.*, 2021, **23**, 5887–5895; (c) N. Salameh, F. Ferlin, F. Valentini, I. Anastasiou and L. Vaccaro, *ACS Sustainable Chem. Eng.*, 2022, **10**, 3766–3776; (d) F. Campana, F. Valentini, A. Marrocchi and L. Vaccaro, *Biofuel Res. J.*, 2023, **10**, 1989–1998; (e) F. Ferlin, F. Valentini, A. Marrocchi and L. Vaccaro, *ACS Sustainable Chem. Eng.*, 2021, **9**, 9604–9624.

15 (a) V. Facchinetti, C. R. B. Gomes and M. V. N. de Souza, *Tetrahedron*, 2021, **102**, 132544; (b) R. Connon, B. Roche, B. V. Rokade and P. J. Guiry, *Chem. Rev.*, 2021, **121**, 6373–6521; (c) D. Lu, J. Cui, S. Yang and Y. Gong, *ACS Catal.*, 2021, **11**, 4288–4293; (d) L. Ju, Q. Lin, N. J. LiBretto, C. L. Wagner, C. T. Hu, J. T. Miller and T. Diao, *J. Am. Chem. Soc.*, 2021, **143**, 14458–14463; (e) S. R. Shinde, S. N. Inamdar, M. Shinde, C. Pawar, B. Kushwaha, V. A. Obakachi, A. Kajee, R. Chauhan and R. Karpoormath, *J. Mol. Struct.*, 2023, **1273**, 134243; (f) X. Yu, Y. Zhang, Y. Liu, Y. Li and Q. Wang, *J. Agric. Food Chem.*, 2019, **67**, 4224–4231; (g) M. Zhou, W. Jiang, J. Xie, W. Zhang, Z. Ji, J. Zou, Z. Cong, X. Xiao, J. Gu and R. Liu, *ChemMedChem*, 2020, **16**, 309–315; (h) M. Zhou, Y. Qian, J. Xie, W. Zhang, W. Jiang, X. Xiao, S. Chen, C. Dai, Z. Cong, Z. Ji, N. Shao, L. Liu, Y. Wu and R. Liu, *Angew. Chem., Int. Ed.*, 2020, **59**, 6412–6419; (i) W. Jiang, M. Zhou, Z. Cong, J. Xie, W. Zhang, S. Chen, J. Zou, Z. Ji, N. Shao, X. Chen, M. Li and R. Liu, *Angew. Chem.*, 2022, **134**, e202200778.

16 (a) K. A. Jadhav, S. D. Bhosle, S. V. Itage, R. S. Bhosale, G. Eppa and J. S. Yadav, *Tetrahedron Lett.*, 2022, **106**, 154048; (b) M. Trose, F. Lazreg, M. Lesieur and C. S. Cazin, *J. Org. Chem.*, 2015, **80**, 9910–9914; (c) V. Mirkhani, M. Moghadam, S. Tangestaninejad, I. Mohammadpoor-Baltork and M. Mahdavi, *Monatsh. Chem.*, 2009, **140**, 1489–1494; (d) A. Cwik, Z. Hell, A. Hegedüs, Z. Finta and Z. Horváth, *Tetrahedron Lett.*, 2002, **43**, 3985–3987; (e) L. Wang, B. Guo, H.-X. Li, Q. Li, H.-Y. Li and J.-P. Lang, *Dalton Trans.*, 2013, **42**, 15570.

17 (a) M. Ishihara and H. Togo, *Tetrahedron*, 2007, **63**, 1474–1480; (b) H. Fujioka, K. Murai, Y. Ohba, A. Hiramatsu and Y. Kita, *Tetrahedron Lett.*, 2005, **46**, 2197–2199; (c) S. Sayama, *Synlett*, 2006, 1479–1484; (d) N. Karade, G. Tiwari and S. Gampawar, *Synlett*, 2007, 1921–1924; (e) W. Wei, R. Li, N. Huber, G. Kizilsavas, C. T. Ferguson, K. Landfester and K. A. Zhang, *ChemCatChem*, 2021, **13**, 3410–3413.

18 (a) H. Wang, J. Zhang, J. Tan, L. Xin, Y. Li, S. Zhang and K. Xu, *Org. Lett.*, 2018, **20**, 2505–2508; (b) F. Lu, J. Xu, H. Li, K. Wang, D. Ouyang, L. Sun, M. Huang, J. Jiang, J. Hu, H. Alhumade, L. Lu and A. Lei, *Green Chem.*, 2021, **23**, 7982; (b) C. Uma Maheswari, G. Satish Kumar and M. Venkateshwar, *RSC Adv.*, 2014, **4**, 39897–39900; (c) M. Ishihara and H. Togo, *Tetrahedron*, 2007, **63**, 1474–1480; (d) A. Alhalib, S. Kamouka and W. J. Moran, *Org. Lett.*, 2015, **17**, 1453; (e) F. Glorius and K. Schwendieck, *Synthesis*, 2006, 2996; (f) W. Wei, R. Li, N. Huber, G. Kizilsavas, C. T. J. Ferguson, K. Landfester and K. A. I. Zhang, *ChemCatChem*, 2021, **13**, 3410; (g) N. N. Karade, G. B. Tiwari and S. V. Gampawar, *Synlett*, 2007, 1921.

19 L. J. Müller, A. Kätelhön, S. Bringezu, S. McCoy, S. Suh, R. Edwards, V. Sick, S. Kaiser, R. Cuéllar-Franca, A. El Khamlich, J. H. Lee, N. von der Assen and A. Bardow, *Energy Environ. Sci.*, 2020, **13**, 2979–2992.

20 <https://www.climateaction.org/news/carbon-footprint-of-recycled-aluminium>.

21 (a) X. Lu, Z. Zhang, T. Hiraki, O. Takeda, H. Zhu, K. Matsubae and T. Nagasaka, *Nature*, 2022, **606**, 511–515; (b) S. Kosai, K. Matsui, K. Matsubae, E. Yamasue and T. Nagasaka, *Resour., Conserv. Recycl.*, 2021, **166**, 105256; (c) J. M. Cullen and J. M. Allwood, *Environ. Sci. Technol.*, 2013, **47**, 3057–3064; (d) D. Raabe, D. Ponge, P. J. Uggowitzer, M. Roscher, M. Paolantonio, C. Liu, H. Antrekowitsch, E. Kozeschnik, D. Seidmann, B. Gault, F. De Geuser, A. Deschamps, C. Hutchinson, C. Liu, Z. Li, P. Prangnell, J. Robson, P. Shanthraj, S. Vakili, C. Sinclair, L. Bourgeois and S. Pogatscher, *Prog. Mater. Sci.*, 2022, **128**, 100947.

22 (a) P. Nuss and M. J. Eckelman, *PLoS One*, 2014, **9**, e101298; (b) J. Torrubia, A. Valero and A. Valero, *Resour., Conserv. Recycl.*, 2023, **199**, 107281.

23 <https://worldsteel.org/steel-topics/sustainability/sustainability-indicators-2023-report/>.

24 (a) P. Zhou and T. Xu, *ChemComm*, 2020, **56**, 8194–8197; (b) K. S. Yoo, C. P. Park, C. H. Yoon, S. Sakaguchi, J. O'Neil and K. W. Jung, *Org. Lett.*, 2007, **9**, 3933–3935; (c) W. L. Lyon and D. W. MacMillan, *J. Am. Chem. Soc.*, 2023, **145**, 7736–7742; (d) L. Zhao, X. Lu and W. Xu, *J. Org. Chem.*, 2005, **70**, 4059–4063; (e) A. J. Hallett, T. M. O'Brien, E. Carter, B. M. Kariuki, D. M. Murphy and B. D. Ward, *Inorg. Chim. Acta*, 2016, **441**, 86–94.

25 Literature process for *E*-factor comparison in order of appearance in Scheme 3: (a) F. Lu, J. Xu, H. Li, K. Wang, D. Ouyang, L. Sun, M. Huang, J. Jiang, J. Hu, H. Alhumade, L. Lu and A. Lei, *Green Chem.*, 2021, **23**, 7982; (b) C. Uma Maheswari, G. Satish Kumar and M. Venkateshwar, *RSC Adv.*, 2014, **4**, 39897–39900; (c) M. Ishihara and H. Togo, *Tetrahedron*, 2007, **63**, 1474–1480; (d) A. Alhalib, S. Kamouka and W. J. Moran, *Org. Lett.*, 2015, **17**, 1453; (e) F. Glorius and K. Schwendieck, *Synthesis*, 2006, 2996; (f) W. Wei, R. Li, N. Huber, G. Kizilsavas, C. T. J. Ferguson, K. Landfester and K. A. I. Zhang, *ChemCatChem*, 2021, **13**, 3410; (g) N. N. Karade, G. B. Tiwari and S. V. Gampawar, *Synlett*, 2007, 1921.

